Proximal Point-Like Method for Updating Simultaneously Mass and Stiffness Matrices of Finite Element Model

*DAI Hua**, *WANG Kangkang*

College of Science, Nanjing University of Aeronautics and Astronautics, Nanjing 211106, P.R. China

(Received 10 December 2019; revised 15 January 2020; accepted 18 January 2020)

Abstract: The problem of correcting simultaneously mass and stiffness matrices of finite element model of undamped structural systems using vibration tests is considered in this paper. The desired matrix properties, including satisfaction of the characteristic equation, symmetry, positive semidefiniteness and sparsity, are imposed as side constraints to form the optimal matrix pencil approximation problem. Using partial Lagrangian multipliers, we transform the nonlinearly constrained optimization problem into an equivalent matrix linear variational inequality, develop a proximal point-like method for solving the matrix linear variational inequality, and analyze its global convergence. Numerical results are included to illustrate the performance and application of the proposed method.

Key words: model updating; proximal point method; optimal matrix pencil approximation; matrix linear variational inequality

CLC number: O241;O327;TB123 **Document code:** A **Article ID:** 1005-1120(2020)01-0001-12

0 Introduction

It is necessary to build highly accurate mathematical models for analyzing, predicting and controlling the dynamic response of actual structures, such as automobiles, aircrafts, satellites and so on. The analytical model of an undamped system with n degrees of freedom, obtained by finite element methods, can be represented by

$$\boldsymbol{M}_a\ddot{\boldsymbol{x}}(t)+\boldsymbol{K}_a\boldsymbol{x}(t)=\boldsymbol{f}(t) \tag{1}$$

where $\boldsymbol{x}(t)$, $\boldsymbol{f}(t)\in \mathrm{R}^n$ are the displacement and external force vectors, respectively, and $\boldsymbol{M}_a$, $\boldsymbol{K}_a\in \mathrm{R}^{n\times n}$ are the analytical mass and stiffness matrices. In general, $\boldsymbol{M}_a$ and $\boldsymbol{K}_a$ are symmetric, sparse and positive semidefinite matrices (denoted by $\boldsymbol{M}_a\geqslant 0$, $\boldsymbol{K}_a\geqslant 0$) with special zero/nonzero patterns. The natural frequency ω and the corresponding mode shape $\boldsymbol{x}$ of the system can be obtained via the following characteristic equation or generalized eigenvalue problem

$$\boldsymbol{K}_a\boldsymbol{x}=\omega^2\boldsymbol{M}_a\boldsymbol{x} \tag{2}$$

Using eigensolvers[1], we can compute the frequencies $\omega_i^{(a)}$ and the corresponding mode shapes $x_i^{(a)}$ of the finite element model (1). On the other hand, some of the lower order frequencies $\omega_i^{(e)}$ ($i=1,\cdots,m\ll n$) and corresponding mode shapes $x_i^{(e)}$ of the real structure can be obtained experimentally by performing vibration tests on the structure. Owing to the complexity of the actual structure, the finite element model is an approximate discrete analytical model of the continuous structure. The analytically evaluated dynamic behavior of the structure seldom agrees with the corresponding experimentally measured ones. The engineer would like to correct the mass and stiffness matrices of the existing structure such that the updated finite element model predicts accurately the observed dynamic behavior. Then the improved finite element model may be considered to be a better representation of the structure than the original finite element model, and can be used with more confidence to analyze, predict and control the dynamic responses of the structure.

*Corresponding author, E-mail address: hdai@nuaa.edu.cn.

How to cite this article: DAI Hua, WANG Kangkang. Proximal point-like method for updating simultaneously mass and stiffness matrices of finite element model[J]. Transactions of Nanjing University of Aeronautics and Astronautics, 2020,37(1): 1-12.

http://dx.doi.org/10.16356/j.1005-1120.2020.01.001

Over the past years, many methods[2-3] have been developed for correcting finite element model to predict test results more accurately. The most common approach is to correct the analytical mass or stiffness matrix with minimal deviation from the finite element model by imposing the characteristic equation and the desired matrix properties as side constraints.

Assume that the analytical mass matrix $\boldsymbol{M}_a$ is exact. Imposing the characteristic equation and the symmetry of the stiffness matrix as side constraints, Baruch[4] and Wei[5] obtained closed-form solutions of the updated stiffness matrix by using Lagrangian multipliers. However, these methods do not guarantee the positive semidefiniteness of the updated stiffness matrix. Based on the QR-factorization of measured mode shapes, Dai[6] proposed an expression of the updated stiffness matrix. Using a decomposition of the stiffness matrix, Kenigsbuch et al.[7] presented the closed-form solution of the updated stiffness matrix. The stiffness matrices corrected by these two methods not only satisfy the characteristic equation and are symmetric positive semidefinite. In all the aforementioned methods, however, the analytical stiffness matrix is adjusted globally, and the sparsity or the zero/nonzero pattern of the stiffness matrix is not taken into consideration. Kabe[8], Sako and Kabe[9] developed a method and its direct least-squares formulation for updating stiffness matrix by imposing the characteristic equation, the symmetry and connectivity of the stiffness matrix as side constraints. Applying the theory of inverse problems for symmetric matrices[10-11], Li et al.[12] presented a method for updating stiffness elements in local error model. But these methods fail to guarantee that the updated stiffness matrix is positive semidefinite. Recently, Yuan[13-15] considered the problem of finding the least change adjustment to the analytical stiffness matrix subject to constraints including characteristic equation, symmetry, positive semidefiniteness and sparsity of the stiffness matrix, transformed the problem into the dual problem and the matrix linear variational inequality, and presented a subgradient method, a projection and contraction method, and a proximal-point method, respectively.

Using experimentally measured mode shapes, Berman et al.[16] sought the least change adjustment to the analytical mass matrix subject to both the symmetry of the mass matrix and the orthogonality relation, and derived an expression of the updated mass matrix by using Lagrangian multipliers. Zhang[17], and Lee et al.[18] obtained the explicit expressions of the updated mass matrix by using matrix transformation method and the Moore-Penrose inverse, respectively. However, the mass matrices corrected by these expressions not only change the sparsity of the analytical mass matrix, but also are not necessarily positive semidefinite. In order to maintain the sparse structure of the analytical mass matrix, Wei and Zhang[19], and Cha[20] proposed the analytical mass matrix modification method via element correction, but the updated mass matrix fails to be positive semidefinite. Recently, Dai and Wei[21] considered the problem of correcting the analytical mass matrix subject to constraints including symmetry, orthogonality relation, positive semidefiniteness and sparsity of the mass matrix, and presented a cyclic projection method.

Combining the analytical mass matrix modification with the analytical stiffness matrix adjustment, Baruch[22], Berman and Nagy[23], Kenigsbuch and Halevi[7], Cha and Gu[24], Wang and Yang[25] proposed procedures to adjust alternately analytical mass and stiffness matrices. The mass and stiffness matrices are related by the characteristic equation, therefore it is conceivable that simultaneously correcting the mass and stiffness matrices will yield better results than sequential correction. Dai[26], Wei[27], Kenigsbuch and Halevi[7] considered the problem of simultaneously updating the analytical mass and stiffness matrices. However, the analytical mass and stiffness matrices are adjusted globally in these methods. Recently, Yuan and Dai[28] investigated the problem of simultaneously correcting the analytical mass and stiffness matrices to satisfy characteristic equation, symmetry, positive semidefiniteness, orthogonality and sparsity, and presented a subgradient algorithm for solving the problem. However, the computational cost of the subgradient algorithm is expensive and the measured mode shapes may not satisfy orthogonality before the mass matrix is determined. More recently, Wang and Dai[29] developed an alternating projection method for simultaneously correcting the analytical mass and stiffness matrices. Using the vectorization and the Kronecker product of matrices, Rakshit and Khare[30] proposed a novel solution approach for the finite element model updating problem with no spillover. The approach preserves symmetric band structure of finite element model, but fails to guarantee that the updated mass and stiffness matrices are positive semidefinite.

For convenience, we use the following notations. For a matrix $\boldsymbol{A}$, $\mathrm{tr}(\boldsymbol{A})$, $\boldsymbol{A}^{\mathrm{T}}$ and $\|\boldsymbol{A}\|_2$ denote the trace, transpose and spectral norm of $\boldsymbol{A}$, respectively. For $\boldsymbol{A}$, $\boldsymbol{B}\in\mathrm{R}^{n\times m}$, $\langle \boldsymbol{A},\boldsymbol{B}\rangle = \mathrm{tr}(\boldsymbol{B}^{\mathrm{T}}\boldsymbol{A})$ and $\boldsymbol{A}2\boldsymbol{B}$ denote the inner product and the Hadamard product of $\boldsymbol{A}$ and $\boldsymbol{B}$, respectively, and the matrix norm $\|\boldsymbol{A}\|_{\mathrm{F}}$ is the Frobenius norm induced by the inner product. $\boldsymbol{SR}^{n\times n}$ denotes the set of all $n\times n$ symmetric matrices and $\boldsymbol{SR}_0^{n\times n}$ is the set of all symmetric positive semidefinite matrices in $\mathrm{R}^{n\times n}$. $\boldsymbol{A}\geqslant 0$ means that $\boldsymbol{A}$ is a real symmetric positive semidefinite matrix. The vector inequality $\boldsymbol{x}\geqslant 0$ is meant to be componentwise (i.e., for $\boldsymbol{x}=(x_1, x_2,\cdots,x_n)^{\mathrm{T}}\in\mathrm{R}^n$, we write $\boldsymbol{x}\geqslant 0$ if $x_i\geqslant 0$ for all $i=1,\cdots,n$), and let $\mathrm{R}^n_+=\{\boldsymbol{x}|\boldsymbol{x}\in\mathrm{R}^n,\boldsymbol{x}\geqslant 0\}$. For $\boldsymbol{A}$, $\boldsymbol{B}\in\mathrm{R}^{n\times m}$, $\mathrm{sparse}(\boldsymbol{A}) = \mathrm{sparse}(\boldsymbol{B})$ means that the matrix $\boldsymbol{A}$ has the same zero/nonzero patterns with the matrix $\boldsymbol{B}$. Let $\boldsymbol{\Lambda}_e = \mathrm{diag}((\omega_1^{(e)})^2,\cdots,(\omega_m^{(e)})^2)\in\mathrm{R}^{m\times m}$ consist of m measured frequencies, $\boldsymbol{X}_e=[x_1^{(e)},\cdots,x_m^{(e)}]\in\mathrm{R}^{n\times m}$ consist of m measured mode shapes and be of full column rank. Without loss of generality, we assume that the analytical mass matrix $\boldsymbol{M}_a$ and stiffness matrix $\boldsymbol{K}_a$ are symmetric since

$$\left\|[\boldsymbol{M},\boldsymbol{K}]-[\boldsymbol{M}_a,\boldsymbol{K}_a]\right\|_{\mathrm{F}}^2 = \left\|\boldsymbol{M}-\frac{1}{2}(\boldsymbol{M}_a+\boldsymbol{M}_a^{\mathrm{T}})\right\|_{\mathrm{F}}^2+\left\|\frac{1}{2}(\boldsymbol{M}_a-\boldsymbol{M}_a^{\mathrm{T}})\right\|_{\mathrm{F}}^2+\left\|\boldsymbol{K}-\frac{1}{2}(\boldsymbol{K}_a+\boldsymbol{K}_a^{\mathrm{T}})\right\|_{\mathrm{F}}^2+\left\|\frac{1}{2}(\boldsymbol{K}_a-\boldsymbol{K}_a^{\mathrm{T}})\right\|_{\mathrm{F}}^2$$

holds for $\boldsymbol{M}$, $\boldsymbol{K}\in\boldsymbol{SR}^{n\times n}$.

In this paper, we consider the problem of updating simultaneously the analytical mass and stiffness matrices with requirements of satisfaction of the characteristic equation, the symmetry, the positive semidefiniteness and the sparsity, and formulate such a problem as the following matrix pencil nearness problem

$$\begin{aligned} &\min \frac{1}{2}\left\|[\boldsymbol{M},\boldsymbol{K}]-[\boldsymbol{M}_a,\boldsymbol{K}_a]\right\|_{\mathrm{F}}^2 \\ &\text{s.t. } \boldsymbol{K}\boldsymbol{X}_e=\boldsymbol{M}\boldsymbol{X}_e\boldsymbol{\Lambda}_e \\ &\boldsymbol{M}^{\mathrm{T}}=\boldsymbol{M}\geqslant 0 \\ &\boldsymbol{K}^{\mathrm{T}}=\boldsymbol{K}\geqslant 0 \\ &\mathrm{sparse}(\boldsymbol{M})=\mathrm{sparse}(\boldsymbol{M}_a) \\ &\mathrm{sparse}(\boldsymbol{K})=\mathrm{sparse}(\boldsymbol{K}_a) \end{aligned} \tag{3}$$

Using partial Lagrangian multipliers, we convert the nonlinearly constrained optimization problem (3) into an equivalent matrix linear variational inequality. Applying proximal point algorithm (PPA) for variational inequality problems, we develop a proximal point-like method for solving the problem (3).

The rest of this paper is organized as follows. In Section 1, we transform the sparsity constraints on the mass matrix $\boldsymbol{M}$ and stiffness matrix $\boldsymbol{K}$ into two equality constraints, and give a brief description of PPA for variational inequality problems. In Section 2, we convert the matrix pencil nearness problem (3) into an equivalent matrix linear variational inequality by using partial Lagrangian multipliers. In Section 3, we develop a proximal point-like algorithm for solving the problem (3), and analyze its convergence. In Section 4, three numerical experiments are performed to illustrate the effectiveness and application of the proposed method. Some conclusions are drawn in Section 5.

1 Preliminaries

1.1 Reformulation of problem (3)

We transform the sparsity requirements on the mass matrix $\boldsymbol{M}=(m_{ij})\in\mathrm{R}^{n\times n}$ and the stiffness matrix $\boldsymbol{K}=(k_{ij})\in\mathrm{R}^{n\times n}$ into convenient forms. The zero/nonzero patterns of the matrices $\boldsymbol{M}_a=(m_{ij}^{(a)})\in\mathrm{R}^{n\times n}$ and $\boldsymbol{K}_a=(k_{ij}^{(a)})\in\mathrm{R}^{n\times n}$ may be definitely described as the following index sets

$$I_{\mathrm{spar}}^{\boldsymbol{M}_a}=\{(i,j)|m_{ij}^{(a)}=0;i=1,\cdots,n;j=1,\cdots,n\}$$

$$I_{\text{spar}}^{K_a}=\{(i,j)|k_{ij}^{(a)}=0;i=1,\cdots,n;j=1,\cdots,n\}$$

Based on the sparsity constraints on the mass matrix $\boldsymbol{M}$ and the stiffness matrix $\boldsymbol{K}$ depending on the zero/nonzero patterns of the matrices $\boldsymbol{M}_a$ and $\boldsymbol{K}_a$, We define two auxiliary matrices $T_{M_a}=(t_{ij}^{M_a})\in \mathrm{R}^{n\times n}$ and $T_{K_a}=(t_{ij}^{K_a})\in \mathrm{R}^{n\times n}$ as follows

$$t_{ij}^{M_a}=\begin{cases}0 & (i,j)\notin I_{\text{spar}}^{M_a}\\ 1 & (i,j)\in I_{\text{spar}}^{M_a}\end{cases},\quad t_{ij}^{K_a}=\begin{cases}0 & (i,j)\notin I_{\text{spar}}^{K_a}\\ 1 & (i,j)\in I_{\text{spar}}^{K_a}\end{cases}$$

The matrices $\boldsymbol{M}_a$ and $\boldsymbol{K}_a$ are symmetric and so are the matrices T_{Ma} and T_{Ka}. Yuan and Dai[28] showed that

$$\text{sparse}(\boldsymbol{M})=\text{sparse}(\boldsymbol{M}_a)\Leftrightarrow \boldsymbol{M}*\boldsymbol{T}_{M_a}=0$$

$$\text{sparse}(\boldsymbol{K})=\text{sparse}(\boldsymbol{K}_a)\Leftrightarrow \boldsymbol{K}*\boldsymbol{T}_{K_a}=0$$

Then the problem (3) is equivalent to the following convex minimization problem

$$\begin{aligned}&\min \frac{1}{2}\left\|[\boldsymbol{M},\boldsymbol{K}]-[\boldsymbol{M}_a,\boldsymbol{K}_a]\right\|_{\mathrm{F}}^2\\ &\text{s.t.}\ \ \boldsymbol{K}\boldsymbol{X}_e=\boldsymbol{M}\boldsymbol{X}_e\boldsymbol{\Lambda}_e\\ &\qquad \boldsymbol{M},\boldsymbol{K}\in \boldsymbol{SR}_0^{n\times n}\\ &\qquad \boldsymbol{M}*\boldsymbol{T}_{M_a}=0\\ &\qquad \boldsymbol{K}*\boldsymbol{T}_{K_a}=0\end{aligned} \tag{4}$$

Obviously, the feasible region of the problem (4) is nonempty.

In order to convert the minimization problem (4) into an equivalent matrix linear variational inequality, we need the following lemmas.

Lemma 1[31] For following convex programming problem

$$\begin{aligned}&\min f(\boldsymbol{x})\\ &\text{s.t.}\ \ \boldsymbol{x}\in\boldsymbol{\Omega}\end{aligned} \tag{5}$$

where $f(\boldsymbol{x}):\mathrm{R}^n\rightarrow\mathrm{R}$ is a continuously differentiable and convex function and $\boldsymbol{\Omega}\subseteq\mathrm{R}^n$ is a closed convex set, $\boldsymbol{x}^*\in\boldsymbol{\Omega}$ is a minimum if

$$\left\langle \boldsymbol{x}-\boldsymbol{x}^*,\nabla f(\boldsymbol{x}^*)\right\rangle\geqslant 0\qquad \forall \boldsymbol{x}\in\boldsymbol{\Omega} \tag{6}$$

Lemma 2[31] For following constrained minimization problem

$$\begin{aligned}&\min f(\boldsymbol{x})\\ &\text{s.t.}\ \ g_i(\boldsymbol{x})\geqslant 0\quad i=1,\cdots,m\\ &\qquad h_j(\boldsymbol{x})=0\quad j=1,\cdots,l\end{aligned} \tag{7}$$

where $f(\boldsymbol{x})$, $g_i(\boldsymbol{x})$, $h_j(\boldsymbol{x})$: $\mathrm{R}^n\rightarrow\mathrm{R}$ are assumed to be continuously differentiable, its feasible region is denoted by $\boldsymbol{\Omega}$. Let $g(\boldsymbol{x})=(g_1(\boldsymbol{x}),\cdots,g_m(\boldsymbol{x}))^{\mathrm{T}}$, $h(\boldsymbol{x})=(h_1(\boldsymbol{x}),\cdots,h_l(\boldsymbol{x}))^{\mathrm{T}}$, and $L(\boldsymbol{x},\boldsymbol{u},\boldsymbol{v})=f(\boldsymbol{x})-\boldsymbol{u}^{\mathrm{T}}g(\boldsymbol{x})+\boldsymbol{v}^{\mathrm{T}}h(\boldsymbol{x})$ be the Lagrangian function of the minimization problem with Lagrangian multipliers $\boldsymbol{u}\in\mathrm{R}_+^m$ and $\boldsymbol{v}\in\mathrm{R}^l$. Assume that $f(\boldsymbol{x})$, $-g(\boldsymbol{x})$ are convex functions, $h(\boldsymbol{x})$ is a linear function and the minimization problem satisfies the Slater constraint qualification[32], then $\boldsymbol{x}^*\in\boldsymbol{\Omega}$ and $\boldsymbol{u}^*\in\mathrm{R}_+^m$, $\boldsymbol{v}^*\in\mathrm{R}^l$ satisfy the Karush-Kuhn-Tucker (KKT) conditions[31] if and only if

$$L(\boldsymbol{x}^*,\boldsymbol{u},\boldsymbol{v})\leqslant L(\boldsymbol{x}^*,\boldsymbol{u}^*,\boldsymbol{v}^*)\leqslant L(\boldsymbol{x},\boldsymbol{u}^*,\boldsymbol{v}^*) \tag{8}$$

for all $\boldsymbol{x}\in\boldsymbol{\Omega}$, $\boldsymbol{u}\in\mathrm{R}_+^m$ and $\boldsymbol{v}\in\mathrm{R}^l$.

1.2 Proximal point algorithm (PPA)

Let $\boldsymbol{\Omega}\subseteq\mathrm{R}^n$ be a closed convex set, and F: $\mathrm{R}^n\rightarrow\mathrm{R}^n$ be a mapping. Assume that $F(\boldsymbol{u})$ is monotone on $\boldsymbol{\Omega}$, i.e., $\left\langle\boldsymbol{u}-\boldsymbol{v},F(\boldsymbol{u})-F(\boldsymbol{v})\right\rangle\geqslant 0$ for all $\boldsymbol{u}$, $\boldsymbol{v}\in\boldsymbol{\Omega}$. The variational inequality problem is that of finding $\boldsymbol{u}^*\in\boldsymbol{\Omega}$ such that

$$\left\langle\boldsymbol{u}-\boldsymbol{u}^*,F(\boldsymbol{u}^*)\right\rangle\geqslant 0\qquad\forall\boldsymbol{u}\in\boldsymbol{\Omega} \tag{9}$$

A classical method for solving the variational inequality problem is the proximal point algorithm (PPA) proposed first by Martinet[33], and then developed by Rockafellar[34], Burachiky and Iusem[35]. For given $\boldsymbol{u}^k\in\boldsymbol{\Omega}$, the new iterate $\boldsymbol{u}^{k+1}$ is obtained by solving the following auxiliary variational inequality subproblem

$$\begin{aligned}&\boldsymbol{u}^{k+1}\in\boldsymbol{\Omega},\Big\langle\boldsymbol{u}-\boldsymbol{u}^{k+1},F(\boldsymbol{u}^{k+1})+\\ &\beta_k(\boldsymbol{u}^{k+1}-\boldsymbol{u}^k)\Big\rangle\geqslant 0\qquad\forall\boldsymbol{u}\in\boldsymbol{\Omega}\end{aligned} \tag{10}$$

where $\{\beta_k\}$ is a sequence of positive numbers called regularization parameters, bounded above. However, it is impractical to solve exactly the subproblem (10) since solving the subproblem (10) may require a computation as difficult as solving the original problem. Many researchers presented some implementable PPAs. Recently, He et al.[36] proposed an implementable PPA method for monotone variational inequalities. The method generates a proximal point $\tilde{\boldsymbol{u}}^k$ which is the solution of the following proximal subproblem

$$\begin{aligned}&\tilde{\boldsymbol{u}}^k\in\boldsymbol{\Omega},\Big\langle\boldsymbol{u}-\tilde{\boldsymbol{u}}^k,F(\tilde{\boldsymbol{u}}^k)+H(\tilde{\boldsymbol{u}}^k-\boldsymbol{u}^k)\Big\rangle\geqslant 0\\ &\qquad\forall\boldsymbol{u}\in\boldsymbol{\Omega}\end{aligned} \tag{11}$$

where the proximal term $H(\boldsymbol{u})$ is positive definite (not necessarily symmetric) but may not be the gradient of any function, and the new iterate $\boldsymbol{u}^{k+1}$ is updated by

$$\boldsymbol{u}^{k+1}=\boldsymbol{u}^{k}-\alpha_k H(\boldsymbol{u}^{k}-\widetilde{\boldsymbol{u}}^{k}) \tag{12}$$

where

$$\alpha_k^*=\frac{\left\langle \boldsymbol{u}^{k}-\widetilde{\boldsymbol{u}}^{k}, H(\boldsymbol{u}^{k}-\widetilde{\boldsymbol{u}}^{k})\right\rangle}{\left\|H(\boldsymbol{u}^{k}-\widetilde{\boldsymbol{u}}^{k})\right\|_2^2} \tag{13}$$

$$\alpha_k=\gamma\alpha_k^*,\quad \gamma\in[1,2)$$

He et al.[36] established the global convergence of the PPA-based method. The parameter γ in Eq. (13) is a relaxed factor. In practical computation, taking $\gamma\in[1, 2)$ is wise for fast convergence.

2 Equivalent Matrix Linear Variational Inequality Formulation

Let

$$\boldsymbol{\Omega}=\boldsymbol{SR}_0^{\,n\times n}\times\boldsymbol{SR}_0^{\,n\times n}\times\mathrm{R}^{m\times n}\times\mathrm{R}^{n\times n}\times\mathrm{R}^{n\times n}$$

then $\boldsymbol{\Omega}$ is a closed convex set. Let $\boldsymbol{\Delta}\in\mathrm{R}^{m\times n}$, $\boldsymbol{\Gamma}_1$, $\boldsymbol{\Gamma}_2\in\mathrm{R}^{n\times n}$ be the Lagrangian multiplier matrices corresponding to $\boldsymbol{K}\boldsymbol{X}_e=\boldsymbol{M}\boldsymbol{X}_e\boldsymbol{\Lambda}_e$, $\boldsymbol{M}*T_{Ma}=0$ and $\boldsymbol{K}*T_{Ka}=0$, respectively. We get the following partial Lagrangian function for the problem (4)

$$L(\boldsymbol{M},\boldsymbol{K},\boldsymbol{\Delta},\boldsymbol{\Gamma}_1,\boldsymbol{\Gamma}_2)=\frac{1}{2}\left\|\boldsymbol{M}-\boldsymbol{M}_a\right\|_F^2+\frac{1}{2}\left\|\boldsymbol{K}-\boldsymbol{K}_a\right\|_F^2-\mathrm{tr}(\boldsymbol{\Delta}(\boldsymbol{K}\boldsymbol{X}_e-\boldsymbol{M}\boldsymbol{X}_e\boldsymbol{\Lambda}_e))-\mathrm{tr}(\boldsymbol{\Gamma}_1(\boldsymbol{M}*T_{M_a}))-\mathrm{tr}(\boldsymbol{\Gamma}_2(\boldsymbol{K}*T_{K_a})) \tag{14}$$

Eq.(14) is defined on $\boldsymbol{\Omega}$. Obviously, the gradient of $L(\boldsymbol{M},\boldsymbol{K},\boldsymbol{\Delta},\boldsymbol{\Gamma}_1,\boldsymbol{\Gamma}_2)$ with respect to $\boldsymbol{M},\boldsymbol{K},\boldsymbol{\Delta},\boldsymbol{\Gamma}_1$ and $\boldsymbol{\Gamma}_2$ can be written as

$$\begin{cases}\dfrac{\partial L}{\partial \boldsymbol{M}}=\boldsymbol{M}-\boldsymbol{M}_a+\boldsymbol{\Delta}^{\mathrm{T}}\left(\boldsymbol{X}_e\boldsymbol{\Lambda}_e\right)^{\mathrm{T}}-\boldsymbol{\Gamma}_1^{\mathrm{T}}* \\ \dfrac{\partial L}{\partial \boldsymbol{K}}=\boldsymbol{K}-\boldsymbol{K}_a-\boldsymbol{\Delta}^{\mathrm{T}}\boldsymbol{X}_e^{\ \mathrm{T}}-\boldsymbol{\Gamma}_2^{\mathrm{T}}*T_{K_a} \\ \dfrac{\partial L}{\partial \boldsymbol{\Delta}}=-(\boldsymbol{K}\boldsymbol{X}_e-\boldsymbol{M}\boldsymbol{X}_e\boldsymbol{\Lambda}_e)^{\mathrm{T}} \\ \dfrac{\partial L}{\partial \boldsymbol{\Gamma}_1}=-(\boldsymbol{M}*T_{M_a})^{\mathrm{T}} \\ \dfrac{\partial L}{\partial \boldsymbol{\Gamma}_2}=-(\boldsymbol{K}*T_{K_a})^{\mathrm{T}}\end{cases}$$

Let $(\boldsymbol{M}^*, \boldsymbol{K}^*, \boldsymbol{\Delta}^*, \boldsymbol{\Gamma}_1^*, \boldsymbol{\Gamma}_2^*)\in\boldsymbol{\Omega}$ be the KKT point of the problem (4). By Lemma 1 and Lemma 2, noting that $\boldsymbol{M}^*$ and $\boldsymbol{K}^*$ are the minimum points of $L(\boldsymbol{M}, \boldsymbol{K}, \boldsymbol{\Delta}, \boldsymbol{\Gamma}_1, \boldsymbol{\Gamma}_2)$ with respect to $\boldsymbol{M}$ and $\boldsymbol{K}$, respectively, while $\boldsymbol{\Delta}^*$, $\boldsymbol{\Gamma}_1^*$ and $\boldsymbol{\Gamma}_2^*$ are the maximum points of $L(\boldsymbol{M}, \boldsymbol{K}, \boldsymbol{\Delta}, \boldsymbol{\Gamma}_1, \boldsymbol{\Gamma}_2)$ with respect to $\boldsymbol{\Delta}$, $\boldsymbol{\Gamma}_1$, $\boldsymbol{\Gamma}_2$, respectively, we have

$$\begin{cases}\left\langle \boldsymbol{M}-\boldsymbol{M}^*, \boldsymbol{M}^*-\boldsymbol{M}_a+(\boldsymbol{\Delta}^*)^{\mathrm{T}}(\boldsymbol{X}_e\boldsymbol{\Lambda}_e)^{\mathrm{T}}-(\boldsymbol{\Gamma}_1^*)^{\mathrm{T}}*T_{M_a}\right\rangle\geqslant 0 \\ \left\langle \boldsymbol{K}-\boldsymbol{K}^*, \boldsymbol{K}^*-\boldsymbol{K}_a-(\boldsymbol{\Delta}^*)^{\mathrm{T}}(\boldsymbol{X}_e)^{\mathrm{T}}-(\boldsymbol{\Gamma}_2^*)^{\mathrm{T}}*T_{K_a}\right\rangle\geqslant 0 \\ \left\langle \boldsymbol{\Delta}-\boldsymbol{\Delta}^*, (\boldsymbol{K}^*\boldsymbol{X}_e-\boldsymbol{M}^*\boldsymbol{X}_e\boldsymbol{\Lambda}_e)^{\mathrm{T}}\right\rangle\geqslant 0 \\ \left\langle \boldsymbol{\Gamma}_1-\boldsymbol{\Gamma}_1^*, (\boldsymbol{M}^*)^{\mathrm{T}}*T_{M_a}\right\rangle\geqslant 0 \\ \left\langle \boldsymbol{\Gamma}_2-\boldsymbol{\Gamma}_2^*, (\boldsymbol{K}^*)^{\mathrm{T}}*T_{K_a}\right\rangle\geqslant 0 \\ \forall(\boldsymbol{M},\boldsymbol{K},\boldsymbol{\Delta},\boldsymbol{\Gamma}_1,\boldsymbol{\Gamma}_2)\in\boldsymbol{\Omega}\end{cases} \tag{15}$$

The compact form of Eq.(15) is the following linear variational inequality

$$\boldsymbol{u}^*\in\boldsymbol{\Omega}, \left\langle \boldsymbol{u}-\boldsymbol{u}^*, F(\boldsymbol{u}^*)\right\rangle\geqslant 0\quad \forall\boldsymbol{u}\in\boldsymbol{\Omega} \tag{16}$$

where

$$\boldsymbol{u}=\begin{pmatrix}\boldsymbol{M}\\ \boldsymbol{K}\\ \boldsymbol{\Delta}\\ \boldsymbol{\Gamma}_1\\ \boldsymbol{\Gamma}_2\end{pmatrix}, \boldsymbol{u}^*=\begin{pmatrix}\boldsymbol{M}^*\\ \boldsymbol{K}^*\\ \boldsymbol{\Delta}^*\\ \boldsymbol{\Gamma}_1^*\\ \boldsymbol{\Gamma}_2^*\end{pmatrix}$$

$$F(\boldsymbol{u})=\begin{pmatrix}\boldsymbol{M}-\boldsymbol{M}_a+\boldsymbol{\Delta}^{\mathrm{T}}\left(\boldsymbol{X}_e\boldsymbol{\Lambda}_e\right)^{\mathrm{T}}-\boldsymbol{\Gamma}_1^{\mathrm{T}}*T_{M_a}\\ \boldsymbol{K}-\boldsymbol{K}_a-\boldsymbol{\Delta}^{\mathrm{T}}\boldsymbol{X}_e^{\ \mathrm{T}}-\boldsymbol{\Gamma}_2^{\mathrm{T}}*T_{K_a}\\ (\boldsymbol{K}\boldsymbol{X}_e-\boldsymbol{M}\boldsymbol{X}_e\boldsymbol{\Lambda}_e)^{\mathrm{T}}\\ \boldsymbol{M}^{\mathrm{T}}*T_{M_a}\\ \boldsymbol{K}^{\mathrm{T}}*T_{K_a}\end{pmatrix} \tag{17}$$

We call the problem (16) matrix linear variational inequality (MLVI).

3 Proximal Point-Like Method for MLVI

The PPA for linear variational inequalities can be directly extended to the matrix linear variational inequality (16). For given $\boldsymbol{u}^k=\begin{pmatrix}\boldsymbol{M}^k\\ \boldsymbol{K}^k\\ \boldsymbol{\Delta}^k\\ \boldsymbol{\Gamma}_1^k\\ \boldsymbol{\Gamma}_2^k\end{pmatrix}\in\boldsymbol{\Omega}$, the new iterate $\widetilde{\boldsymbol{u}}^k=\begin{pmatrix}\widetilde{\boldsymbol{M}}^k\\ \widetilde{\boldsymbol{K}}^k\\ \widetilde{\boldsymbol{\Delta}}^k\\ \widetilde{\boldsymbol{\Gamma}}_1^k\\ \widetilde{\boldsymbol{\Gamma}}_2^k\end{pmatrix}$ is obtained by solving the following proximal subproblem

$$\widetilde{\boldsymbol{u}}^k \in \boldsymbol{\Omega}, \left\langle \boldsymbol{u} - \widetilde{\boldsymbol{u}}^k, F(\widetilde{\boldsymbol{u}}^k) + H(\widetilde{\boldsymbol{u}}^k - \boldsymbol{u}^k) \right\rangle \geqslant 0 \quad \forall \boldsymbol{u} \in \boldsymbol{\Omega} \tag{18}$$

where $H(\widetilde{\boldsymbol{u}}^k - \boldsymbol{u}^k)$ is the proximal term. In this paper, we construct the proximal term as follows

$$H(\boldsymbol{u}) = \begin{pmatrix} r_1 \boldsymbol{M} + \boldsymbol{\Delta}^{\mathrm{T}} \left(\boldsymbol{X}_e \boldsymbol{\Lambda}_e \right)^{\mathrm{T}} - \boldsymbol{\Gamma}_1^{\mathrm{T}} * T_{M_a} \\ r_2 \boldsymbol{K} - \boldsymbol{\Delta}^{\mathrm{T}} \boldsymbol{X}_e^{\mathrm{T}} - \boldsymbol{\Gamma}_2^{\mathrm{T}} * T_{K_a} \\ s\boldsymbol{\Delta} - (\boldsymbol{K}\boldsymbol{X}_e - \boldsymbol{M}\boldsymbol{X}_e \boldsymbol{\Lambda}_e)^{\mathrm{T}} \\ t_1 \boldsymbol{\Gamma}_1 - \boldsymbol{M}^{\mathrm{T}} * T_{M_a} \\ t_2 \boldsymbol{\Gamma}_2 - \boldsymbol{K}^{\mathrm{T}} * T_{K_a} \end{pmatrix} \tag{19}$$

where $\boldsymbol{u} \in \boldsymbol{\Omega}$ and s, $r_i, t_i \in \mathrm{R}$ $(i = 1, 2)$ are positive numbers selected to ensure the positive definiteness of the linear operator $H(\boldsymbol{u})$.

It is easy to verify the following lemma.

Lemma 3 Let A, $B \in \mathrm{R}^{m \times n}$, $\boldsymbol{C}$, $\boldsymbol{D} \in \mathrm{R}^{n \times n}$, $\boldsymbol{S} \in \boldsymbol{SR}^{n \times n}$. Then

(1) $\mathrm{tr}(\boldsymbol{A}^{\mathrm{T}}\boldsymbol{B}) = \mathrm{tr}(\boldsymbol{B}^{\mathrm{T}}\boldsymbol{A})$;

(2) $\left|\langle A, B \rangle\right| \leqslant \|A\|_{\mathrm{F}} \|B\|_{\mathrm{F}} \leqslant \frac{1}{2}\left(\|A\|_{\mathrm{F}}^2 + \|B\|_{\mathrm{F}}^2 \right)$;

(3) $\mathrm{tr}(\boldsymbol{C}(\boldsymbol{D}*\boldsymbol{S})) = \mathrm{tr}(\boldsymbol{D}(\boldsymbol{C}*\boldsymbol{S}))$.

Theorem 1 For any $\boldsymbol{u}$, $\boldsymbol{v} \in \boldsymbol{\Omega}$, $\left\langle \boldsymbol{u} - \boldsymbol{v}, F(\boldsymbol{u}) - F(\boldsymbol{v}) \right\rangle \geqslant 0$ holds.

Proof For any $\boldsymbol{u} = \begin{pmatrix} \boldsymbol{M} \\ \boldsymbol{K} \\ \boldsymbol{\Delta} \\ \boldsymbol{\Gamma}_1 \\ \boldsymbol{\Gamma}_2 \end{pmatrix}, \boldsymbol{v} = \begin{pmatrix} \boldsymbol{M}' \\ \boldsymbol{K}' \\ \boldsymbol{\Delta}' \\ \boldsymbol{\Gamma}_1' \\ \boldsymbol{\Gamma}_2' \end{pmatrix} \in \boldsymbol{\Omega}$, it follows from Lemma 3 that

$$\left\langle \boldsymbol{u} - \boldsymbol{v}, F(\boldsymbol{u}) - F(\boldsymbol{v}) \right\rangle = \mathrm{tr}\left[(\boldsymbol{u} - \boldsymbol{v})^{\mathrm{T}} (F(\boldsymbol{u}) - F(\boldsymbol{v})) \right] = \|\boldsymbol{M} - \boldsymbol{M}'\|_{\mathrm{F}}^2 + \|\boldsymbol{K} - \boldsymbol{K}'\|_{\mathrm{F}}^2 \geqslant 0$$

Theorem 1 shows that the mapping F defined by Eq.(17) is monotone.

Theorem 2 (1) For any $\boldsymbol{u}$, $\boldsymbol{v} \in \boldsymbol{\Omega}$, $\left\langle \boldsymbol{u}, H(\boldsymbol{v}) \right\rangle = \left\langle \boldsymbol{v}, H(\boldsymbol{u}) \right\rangle$ holds;

(2) There exists $c > 0$ such that $\left\| H(\boldsymbol{u}) \right\|_{\mathrm{F}}^2 \leqslant c\|\boldsymbol{u}\|_{\mathrm{F}}^2$ for any $\boldsymbol{u} \in \boldsymbol{\Omega}$;

(3) If r_1, r_2, s, t_1, t_2 satisfy

$$r_1 > 1 + 2\left\| \boldsymbol{X}_e \boldsymbol{\Lambda}_e \right\|_2^2, r_2 > 1 + 2\left\| \boldsymbol{X}_e \right\|_2^2 \quad s > 1, t_i > 1 \quad i = 1, 2 \tag{20}$$

then there exists $d > 0$ such that $\left\langle \boldsymbol{u}, H(\boldsymbol{u}) \right\rangle \geqslant d\|\boldsymbol{u}\|_{\mathrm{F}}^2$ for any $\boldsymbol{u} \in \boldsymbol{\Omega}$.

Proof By Lemma 3, it is easy to verify that both (1) and (2) hold. Now, we prove (3). By the definition of the auxiliary matrices T_{M_a} and T_{K_a}, we have $\left\| Y * T_{M_a} \right\|_{\mathrm{F}} \leqslant \|Y\|_{\mathrm{F}}$ and $\left\| Y * T_{K_a} \right\|_{\mathrm{F}} \leqslant \|Y\|_{\mathrm{F}}$ for any $Y \in \mathrm{R}^{n \times n}$. It follows from Lemma 3 that

$$2\left\langle \boldsymbol{\Delta}, (\boldsymbol{K}\boldsymbol{X}_e - \boldsymbol{M}\boldsymbol{X}_e\boldsymbol{\Lambda}_e)^{\mathrm{T}} \right\rangle \leqslant \|\boldsymbol{\Delta}\|_{\mathrm{F}}^2 + \left\| \boldsymbol{K}\boldsymbol{X}_e - \boldsymbol{M}\boldsymbol{X}_e\boldsymbol{\Lambda}_e \right\|_{\mathrm{F}}^2 \leqslant \|\boldsymbol{\Delta}\|_{\mathrm{F}}^2 + \left\| \boldsymbol{K}\boldsymbol{X}_e \right\|_{\mathrm{F}}^2 + \left\| \boldsymbol{M}\boldsymbol{X}_e\boldsymbol{\Lambda}_e \right\|_{\mathrm{F}}^2 + 2\left\| \boldsymbol{K}\boldsymbol{X}_e \right\|_{\mathrm{F}} \times \left\| \boldsymbol{M}\boldsymbol{X}_e\boldsymbol{\Lambda}_e \right\|_{\mathrm{F}} \leqslant \|\boldsymbol{\Delta}\|_{\mathrm{F}}^2 + 2\left\| \boldsymbol{X}_e\boldsymbol{\Lambda}_e \right\|_2^2 \times \|\boldsymbol{M}\|_{\mathrm{F}}^2 + 2\left\| \boldsymbol{X}_e \right\|_2^2 \times \|\boldsymbol{K}\|_{\mathrm{F}}^2$$

$$2\left\langle \boldsymbol{\Gamma}_1, (\boldsymbol{M} * T_{M_a})^{\mathrm{T}} \right\rangle \leqslant \left\| \boldsymbol{\Gamma}_1 \right\|_{\mathrm{F}}^2 + \left\| \boldsymbol{M}^{\mathrm{T}} * T_{M_a} \right\|_{\mathrm{F}}^2 \leqslant \left\| \boldsymbol{\Gamma}_1 \right\|_{\mathrm{F}}^2 + \|\boldsymbol{M}\|_{\mathrm{F}}^2$$

$$2\left\langle \boldsymbol{\Gamma}_2, (\boldsymbol{K} * T_{K_a})^{\mathrm{T}} \right\rangle \leqslant \left\| \boldsymbol{\Gamma}_2 \right\|_{\mathrm{F}}^2 + \left\| \boldsymbol{K}^{\mathrm{T}} * T_{K_a} \right\|_{\mathrm{F}}^2 \leqslant \left\| \boldsymbol{\Gamma}_2 \right\|_{\mathrm{F}}^2 + \|\boldsymbol{K}\|_{\mathrm{F}}^2$$

$$\begin{aligned} \left\langle \boldsymbol{u}, H(\boldsymbol{u}) \right\rangle = {} & r_1\|\boldsymbol{M}\|_{\mathrm{F}}^2 + r_2\|\boldsymbol{K}\|_{\mathrm{F}}^2 + s\|\boldsymbol{\Delta}\|_{\mathrm{F}}^2 + t_1\left\| \boldsymbol{\Gamma}_1 \right\|_{\mathrm{F}}^2 + t_2\left\| \boldsymbol{\Gamma}_2 \right\|_{\mathrm{F}}^2 - \\ & 2\left\langle \boldsymbol{\Delta}, (\boldsymbol{K}\boldsymbol{X}_e - \boldsymbol{M}\boldsymbol{X}_e\boldsymbol{\Lambda}_e)^{\mathrm{T}} \right\rangle - 2\left\langle \boldsymbol{\Gamma}_1, (\boldsymbol{M} * T_{M_a})^{\mathrm{T}} \right\rangle - 2\left\langle \boldsymbol{\Gamma}_2, (\boldsymbol{K} * T_{K_a})^{\mathrm{T}} \right\rangle \geqslant \\ & \left(r_1 - 1 - 2\left\| \boldsymbol{X}_e\boldsymbol{\Lambda}_e \right\|_2^2 \right)\|\boldsymbol{M}\|_{\mathrm{F}}^2 + \left(r_2 - 1 - 2\left\| \boldsymbol{X}_e \right\|_2^2 \right)\|\boldsymbol{K}\|_{\mathrm{F}}^2 + (s-1)\|\boldsymbol{\Delta}\|_{\mathrm{F}}^2 + (t_1 - 1)\left\| \boldsymbol{\Gamma}_1 \right\|_{\mathrm{F}}^2 + (t_2 - 1)\left\| \boldsymbol{\Gamma}_2 \right\|_{\mathrm{F}}^2 \geqslant d\|\boldsymbol{u}\|_{\mathrm{F}}^2 \end{aligned}$$

where $d = \min\{ r_1 - 1 - 2\left\| \boldsymbol{X}_e\boldsymbol{\Lambda}_e \right\|_2^2, r_2 - 1 - 2\left\| \boldsymbol{X}_e \right\|_2^2, s - 1, t_1 - 1, t_2 - 1 \}$. By Eq.(20), we have $d > 0$.

Remark 1 Theorem 2 shows that the linear operator $H(\boldsymbol{u})$ is positive definite on $\boldsymbol{\Omega}$ under the condition (20). For convenience, we use the notation $\|\boldsymbol{u}\|_H^2 := \sqrt{\left\langle \boldsymbol{u}, H(\boldsymbol{u}) \right\rangle}$, and assume that Eq. (20) holds always.

By Eq. (19), we can decompose the problem (18) into several smaller and easier subproblems as follows

$$\left\langle \boldsymbol{M} - \widetilde{\boldsymbol{M}}^k, (r_1 + 1)\widetilde{\boldsymbol{M}}^k - r_1\boldsymbol{M}^k - \boldsymbol{M}_a + (2\widetilde{\boldsymbol{\Delta}}^k - \boldsymbol{\Delta}^k)^{\mathrm{T}}(\boldsymbol{X}_e\boldsymbol{\Lambda}_e)^{\mathrm{T}} - (2\widetilde{\boldsymbol{\Gamma}}_1^k - \boldsymbol{\Gamma}_1^k)^{\mathrm{T}} * T_{M_a} \right\rangle \geqslant 0 \quad \forall \boldsymbol{M} \in \boldsymbol{SR}_0^{n \times n} \tag{21}$$

$$\left\langle \boldsymbol{K} - \widetilde{\boldsymbol{K}}^k, (r_2 + 1)\widetilde{\boldsymbol{K}}^k - r_2\boldsymbol{K}^k - \boldsymbol{K}_a - (2\widetilde{\boldsymbol{\Delta}}^k - \boldsymbol{\Delta}^k)^{\mathrm{T}}\boldsymbol{X}_e^{\mathrm{T}} - (2\widetilde{\boldsymbol{\Gamma}}_2^k - \boldsymbol{\Gamma}_2^k)^{\mathrm{T}} * T_{K_a} \right\rangle \geqslant 0 \quad \forall \boldsymbol{K} \in \boldsymbol{SR}_0^{n \times n} \tag{22}$$

$$\left\langle \boldsymbol{\Delta} - \widetilde{\boldsymbol{\Delta}}^k, s(\widetilde{\boldsymbol{\Delta}}^k - \boldsymbol{\Delta}^k) + (\boldsymbol{K}^k\boldsymbol{X}_e - \boldsymbol{M}^k\boldsymbol{X}_e\boldsymbol{\Lambda}_e)^{\mathrm{T}} \right\rangle \geqslant 0 \quad \forall \boldsymbol{\Delta} \in \mathrm{R}^{m\times n} \tag{23}$$

$$\left\langle \boldsymbol{\Gamma}_1 - \widetilde{\boldsymbol{\Gamma}}_1^k, t_1(\widetilde{\boldsymbol{\Gamma}}_1^k - \boldsymbol{\Gamma}_1^k) + (\boldsymbol{M}^k)^{\mathrm{T}} * \boldsymbol{T}_{M_a} \right\rangle \geqslant 0 \quad \forall \boldsymbol{\Gamma}_1 \in \mathrm{R}^{n\times n} \tag{24}$$

$$\left\langle \boldsymbol{\Gamma}_2 - \widetilde{\boldsymbol{\Gamma}}_2^k, t_2(\widetilde{\boldsymbol{\Gamma}}_2^k - \boldsymbol{\Gamma}_2^k) + (\boldsymbol{K}^k)^{\mathrm{T}} * \boldsymbol{T}_{K_a} \right\rangle \geqslant 0 \quad \forall \boldsymbol{\Gamma}_2 \in \mathrm{R}^{n\times n} \tag{25}$$

It is easy to find the solutions to the problems (23)—(25) as follows

$$\widetilde{\boldsymbol{\Delta}}^k = \boldsymbol{\Delta}^k - \frac{1}{s}(\boldsymbol{K}^k\boldsymbol{X}_e - \boldsymbol{M}^k\boldsymbol{X}_e\boldsymbol{\Lambda}_e)^{\mathrm{T}} \tag{26}$$

$$\widetilde{\boldsymbol{\Gamma}}_1^k = \boldsymbol{\Gamma}_1^k - \frac{1}{t_1}(\boldsymbol{M}^k * \boldsymbol{T}_{M_a})^{\mathrm{T}} \tag{27}$$

$$\widetilde{\boldsymbol{\Gamma}}_2^k = \boldsymbol{\Gamma}_2^k - \frac{1}{t_2}(\boldsymbol{K}^k * \boldsymbol{T}_{K_a})^{\mathrm{T}} \tag{28}$$

The problems (21) and (22) are equivalent to the following minimization problems

$$\min \left\| \boldsymbol{M} - \frac{1}{r_1+1}\left[r_1\boldsymbol{M}^k + \boldsymbol{M}_a - (2\widetilde{\boldsymbol{\Delta}}^k - \boldsymbol{\Delta}^k)^{\mathrm{T}}(\boldsymbol{X}_e\boldsymbol{\Lambda}_e)^{\mathrm{T}} + (2\widetilde{\boldsymbol{\Gamma}}_1^k - \boldsymbol{\Gamma}_1^k)^{\mathrm{T}} * \boldsymbol{T}_{M_a} \right] \right\|_{\mathrm{F}}^2 \quad \text{s.t. } \boldsymbol{M} \in \boldsymbol{SR}_0^{n\times n} \tag{29}$$

$$\min \left\| \boldsymbol{K} - \frac{1}{r_2+1}\left[r_2\boldsymbol{K}^k + \boldsymbol{K}_a + (2\widetilde{\boldsymbol{\Delta}}^k - \boldsymbol{\Delta}^k)^{\mathrm{T}}\boldsymbol{X}_e^{\mathrm{T}} + (2\widetilde{\boldsymbol{\Gamma}}_2^k - \boldsymbol{\Gamma}_2^k)^{\mathrm{T}} * \boldsymbol{T}_{K_a} \right] \right\|_{\mathrm{F}}^2 \quad \text{s.t. } \boldsymbol{K} \in \boldsymbol{SR}_0^{n\times n} \tag{30}$$

In order to find the solutions to the subproblems (29) and (30), we need the following Lemma.

Lemma 4[37] Let $A \in \mathrm{R}^{n\times n}$, $\hat{A} = (A^{\mathrm{T}} + A)/2$, and the spectral decomposition of the real symmetric matrix $\hat{A} = \boldsymbol{Q}\mathrm{diag}(\theta_1, \theta_2, \cdots, \theta_n)\boldsymbol{Q}^{\mathrm{T}}$, where $\theta_j (j = 1, 2, \cdots, n)$ are the eigenvalues of $\hat{A}$, $\boldsymbol{Q} \in \mathrm{R}^{n\times n}$ is an orthogonal matrix. Then the following problem

$$\min \| \boldsymbol{X} - \boldsymbol{A} \|_{\mathrm{F}}^2 \quad \text{s.t. } \boldsymbol{X} \in \boldsymbol{SR}_0^{n\times n}$$

has the unique solution $\boldsymbol{A}_+$ which may be expressed by

$$\boldsymbol{A}_+ = \boldsymbol{Q}\mathrm{diag}(\beta_1, \beta_2, \cdots, \beta_n)\boldsymbol{Q}^{\mathrm{T}}$$

where $\beta_i = \max\{\theta_i, 0\}$, $i = 1, 2, \cdots, n$.

Using Lemma 4, it is easy to compute the solutions to the subproblems (29) and (30), denoted by $\widetilde{\boldsymbol{M}}^k$ and $\widetilde{\boldsymbol{K}}^k$, respectively.

From Theorem 1, we know that the problem (16) is a monotone variational inequality. Once $\widetilde{\boldsymbol{M}}^k, \widetilde{\boldsymbol{K}}^k, \widetilde{\boldsymbol{\Delta}}^k, \widetilde{\boldsymbol{\Gamma}}_1^k$ and $\widetilde{\boldsymbol{\Gamma}}_2^k$ are obtained, $\boldsymbol{u}^k$ can be updated to $\boldsymbol{u}^{k+1}$ by using Eqs.(12), (13) and (19). However, this is time consuming. We use the following extrapolation formula to correct $\boldsymbol{u}^{k+1}$, that is

$$\boldsymbol{u}^{k+1} = \boldsymbol{u}^k - \gamma(\boldsymbol{u}^k - \widetilde{\boldsymbol{u}}^k) \tag{31}$$

where the parameter γ is a relaxed factor, it is wise to set $\gamma \in [1, 2)$ for guaranteeing the fast convergence[38]. A numerical algorithm for the problem (4) is summarized as follows.

Algorithm 1 Proximal point-like algorithm

Input: $\boldsymbol{M}_a, \boldsymbol{K}_a, \boldsymbol{T}_{M_a}, \boldsymbol{T}_{K_a} \in \boldsymbol{SR}^{n\times n}, \boldsymbol{\Lambda}_e \in \mathrm{R}^{m\times m}$, $\boldsymbol{X}_e \in \mathrm{R}^{n\times m}$, initial matrices $\boldsymbol{M}^0$, $\boldsymbol{K}^0 \in \boldsymbol{SR}^{n\times n}$, $\boldsymbol{\Delta}^0 \in \mathrm{R}^{m\times n}$, $\boldsymbol{\Gamma}_1^0, \boldsymbol{\Gamma}_2^0 \in \mathrm{R}^{n\times n}$, tolerance $\varepsilon > 0$ and $k = 0$.

Output: Updated mass and stiffness matrices.

(1) Compute $\widetilde{\boldsymbol{\Delta}}^k, \widetilde{\boldsymbol{\Gamma}}_1^k$ and $\widetilde{\boldsymbol{\Gamma}}_2^k$ by using Eqs. (26), (27) and (28), respectively;

(2) Solve the subproblems (29) and (30) to get $\widetilde{\boldsymbol{M}}^k, \widetilde{\boldsymbol{K}}^k$, respectively;

(3) Compute the new iterate $\boldsymbol{u}^{k+1}$ by using Eq.(31);

(4) If $\|\boldsymbol{u}^k - \widetilde{\boldsymbol{u}}^k\|_{\mathrm{F}} < \varepsilon$, set the solution $\boldsymbol{u}^* = \boldsymbol{u}^{k+1}$ and exit; else set $k := k+1$ and go to (1).

Now we analyze the convergence of Algorithm 1 and show that Algorithm 1 converges globally.

Lemma 5 Let $\boldsymbol{\Omega}^*$ be the solution set of the problem (16) which is assumed to be nonempty, and $\boldsymbol{u}^*$ be a solution of the problem (16). If $\widetilde{\boldsymbol{u}}^k$ is generated from the given $\boldsymbol{u}^k \in \boldsymbol{\Omega}$ by Eq. (18) with the proximal term $H(\boldsymbol{u})$ (Eq.(19)), then

$$\left\langle \boldsymbol{u}^k - \boldsymbol{u}^*, H(\boldsymbol{u}^k - \widetilde{\boldsymbol{u}}^k) \right\rangle \geqslant \|\boldsymbol{u}^k - \widetilde{\boldsymbol{u}}^k\|_H^2 \quad \forall \boldsymbol{u}^* \in \boldsymbol{\Omega}^* \tag{32}$$

Proof Since $\boldsymbol{u}^* \in \boldsymbol{\Omega}^*$, it follows from Eq.(18) and the linearity of $H(\boldsymbol{u})$ that

$$\left\langle \boldsymbol{u}^k - \boldsymbol{u}^*, H(\boldsymbol{u}^k - \widetilde{\boldsymbol{u}}^k) - F(\widetilde{\boldsymbol{u}}^k) \right\rangle \geqslant 0 \tag{33}$$

On the other hand, since $\widetilde{\boldsymbol{u}}^k \in \boldsymbol{\Omega}$, and $\boldsymbol{u}^*$ is a solution of the problem (16), we have

$$\left\langle \widetilde{\boldsymbol{u}}^k - \boldsymbol{u}^*, F(\boldsymbol{u}^*) \right\rangle \geqslant 0 \tag{34}$$

Adding Eqs.(33) and (34) and using Theorem 1, we obtain

$$\left\langle \tilde{\boldsymbol{u}}^k-\boldsymbol{u}^*,H(\boldsymbol{u}^k-\tilde{\boldsymbol{u}}^k)\right\rangle \geqslant \left\langle \tilde{\boldsymbol{u}}^k-\boldsymbol{u}^*,F(\tilde{\boldsymbol{u}}^k)-F(\boldsymbol{u}^*)\right\rangle \geqslant 0 \tag{35}$$

Consequently, we have Eq.(32).

Lemma 6 Let $\tilde{\boldsymbol{u}}^k$ be the proximal point generated from the given $\boldsymbol{u}^k\in\boldsymbol{\Omega}$ by Eq.(18) with the proximal term $H(\boldsymbol{u})$ (Eq.(19)). Then for all $\boldsymbol{u}^*\in\boldsymbol{\Omega}^*$, the sequence $\{\boldsymbol{u}^k\}$ generated by Algorithm 1 satisfies

$$\left\|\boldsymbol{u}^{k+1}-\boldsymbol{u}^*\right\|_H^2 \leqslant \left\|\boldsymbol{u}^k-\boldsymbol{u}^*\right\|_H^2-\gamma(2-\gamma)\left\|\boldsymbol{u}^k-\tilde{\boldsymbol{u}}^k\right\|_H^2 \tag{36}$$

Proof It follows from Theorem 2, Eq.(31) and Lemma 5 that

$$\left\|\boldsymbol{u}^{k+1}-\boldsymbol{u}^*\right\|_H^2=\left\|\boldsymbol{u}^k-\gamma(\boldsymbol{u}^k-\tilde{\boldsymbol{u}}^k)-\boldsymbol{u}^*\right\|_H^2= \left\|\boldsymbol{u}^k-\boldsymbol{u}^*\right\|_H^2-2\gamma\left\langle \boldsymbol{u}^k-\boldsymbol{u}^*,H(\boldsymbol{u}^k-\tilde{\boldsymbol{u}}^k)\right\rangle+ \gamma^2\left\|\boldsymbol{u}^k-\tilde{\boldsymbol{u}}^k\right\|_H^2\leqslant\left\|\boldsymbol{u}^k-\boldsymbol{u}^*\right\|_H^2-\gamma(2-\gamma)\left\|\boldsymbol{u}^k-\tilde{\boldsymbol{u}}^k\right\|_H^2$$

Lemma 6 shows that the sequence $\{\boldsymbol{u}^k\}$ generated by Algorithm 1 is Fejér monotone[39] with respect to the solution set $\boldsymbol{\Omega}^*$.

Theorem 3 The sequence $\{\boldsymbol{u}^k\}$ generated by Algorithm 1 for the problem (16) converges to the solution set $\boldsymbol{\Omega}^*$.

Proof For any $\gamma\in[1,2)$, it follows from Theorem 2 and Lemma 6 that $\{\boldsymbol{u}^k\}$ is bounded and thus

$$\lim_{k\to\infty}\left\|\boldsymbol{u}^k-\tilde{\boldsymbol{u}}^k\right\|_H=0$$

Consequently, $\{\tilde{\boldsymbol{u}}^k\}$ is also bounded. Let $\boldsymbol{u}^\infty$ be an accumulation point of $\{\tilde{\boldsymbol{u}}^k\}$, then there exists a subsequence $\{\tilde{\boldsymbol{u}}^{k_j}\}$ in the sequence $\{\tilde{\boldsymbol{u}}^k\}$ such that $\{\tilde{\boldsymbol{u}}^{k_j}\}$ converges to $\boldsymbol{u}^\infty$. From Eq.(18), we have

$$\tilde{\boldsymbol{u}}^{k_j}\in\boldsymbol{\Omega},\left\langle \boldsymbol{u}-\tilde{\boldsymbol{u}}^{k_j},F(\tilde{\boldsymbol{u}}^{k_j})+H(\tilde{\boldsymbol{u}}^{k_j}-\boldsymbol{u}^{k_j})\right\rangle\geqslant 0 \quad \forall\boldsymbol{u}\in\boldsymbol{\Omega}$$

Since $\tilde{\boldsymbol{u}}^{k_j}\to\boldsymbol{u}^\infty$ and $\lim_{j\to\infty}\|\boldsymbol{u}^{k_j}-\tilde{\boldsymbol{u}}^{k_j}\|_H=0$, we obtain $\boldsymbol{u}^{k_j}\to\boldsymbol{u}^\infty$, and

$$\boldsymbol{u}^\infty\in\boldsymbol{\Omega},\left\langle \boldsymbol{u}-\boldsymbol{u}^\infty,F(\boldsymbol{u}^\infty)\right\rangle\geqslant 0 \quad \forall\boldsymbol{u}\in\boldsymbol{\Omega}$$

and thus $\boldsymbol{u}^\infty$ is a solution point of the problem (16). Noting that the inequality (36) is true for all solutions of the problem (18), we get

$$\left\|\boldsymbol{u}^{k+1}-\boldsymbol{u}^\infty\right\|_H^2\leqslant\left\|\boldsymbol{u}^k-\boldsymbol{u}^\infty\right\|_H^2 \quad \forall k\geqslant 0$$

thus the sequence $\{\boldsymbol{u}^k\}$ converges to $\boldsymbol{u}^\infty$.

4 Numerical Tests

In this section, we present three numerical examples to show the effectiveness and the application of Algorithm 1 for solving the problem (3) arising in structural dynamics model updating. All the numerical tests are carried out in MATLAB. Let $\lambda_i^{(e)}$ and $\boldsymbol{x}_i^{(e)}$ ($i=1,2,\cdots,m$) be the measured lower order eigenvalues and corresponding eigenvectors, respectively, and λ_i and $\boldsymbol{x}_i$ ($i=1,2,\cdots,m$) be the lower order eigenvalues and corresponding eigenvectors of the updated system, respectively. We use $\boldsymbol{M}$ and $\boldsymbol{K}$ to denote the updated mass and stiffness matrices, respectively. Let

$$\mathrm{Err}=\left\|\boldsymbol{K}\boldsymbol{X}_e-\boldsymbol{M}\boldsymbol{X}_e\boldsymbol{\Lambda}_e\right\|_F$$

$$\lambda_i^{(\mathrm{err})}=\left|\lambda_i^{(e)}-\lambda_i\right|$$

$$\theta_i^{(\mathrm{err})}=\arccos\left(\frac{\left\langle x_i^{(e)},x_i\right\rangle}{\left\|x_i^{(e)}\right\|_2\cdot\left\|x_i\right\|_2}\right)$$

$$i=1,2,\cdots,m$$

In Algorithm 1, the parameters r_1, r_2, s, t_1, t_2 in $H(\boldsymbol{u})$ should theoretically satisfy Eq.(20). In fact, the parameter s only needs to satisfy the condition $s>0$ since some inequalities are overestimated in the proof of Theorem 2, so some of our numerical experiments show that Algorithm 1 converges faster for $0<s<1$ than for $s\geqslant 1$.

Example 1 An undamped spring-mass system, including the spring stiffness and mass values, is shown in Fig.1.

Let $m_i=1$ kg ($i=1,2,\cdots,5$), $k_i=0.5$ N/m ($i=1,2,\cdots,6$). The exact stiffness and mass matri-

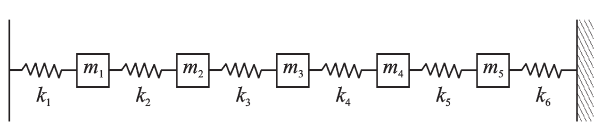

Fig.1 Spring-mass system

ces are given by

$$\hat{M}=\begin{bmatrix}1&0&0&0&0\\0&1&0&0&0\\0&0&1&0&0\\0&0&0&1&0\\0&0&0&0&1\end{bmatrix}$$

$$\hat{K}=\begin{bmatrix}1&-0.5&0&0&0\\-0.5&1&-0.5&0&0\\0&-0.5&1&-0.5&0\\0&0&-0.5&1&-0.5\\0&0&0&-0.5&1\end{bmatrix}$$

We choose three exact lower order eigenvalues and corresponding eigenvectors as the given measured data, denoted by $\boldsymbol{\Lambda}_e$ and $\boldsymbol{X}_e$, respectively.

$$\boldsymbol{\Lambda}_e=\begin{bmatrix}0.134\,0&0&0\\0&0.500\,0&0\\0&0&1.000\,0\end{bmatrix}$$

$$\boldsymbol{X}_e=\begin{bmatrix}-0.288\,7&-0.500\,0&0.577\,4\\-0.500\,0&-0.500\,0&-0.000\,0\\-0.577\,4&0.000\,0&-0.577\,4\\-0.500\,0&0.500\,0&-0.000\,0\\-0.288\,7&0.500\,0&0.577\,4\end{bmatrix}$$

To show the effectiveness of Algorithm 1, the exact stiffness and mass matrices are perturbed by

$$\boldsymbol{M}_a:=\hat{\boldsymbol{M}}+\mu\boldsymbol{R}_M*\hat{\boldsymbol{M}},\ \boldsymbol{K}_a:=\hat{\boldsymbol{K}}+\mu\boldsymbol{R}_K*\hat{\boldsymbol{K}}$$

where $\boldsymbol{R}_M$ and $\boldsymbol{R}_K$ are 5×5 symmetric matrices whose entries are generated randomly and distributed uniformly within $[-1.0, 1.0]$, and μ is a parameter. In this example, we set $\mu=0.001$.

To implement Algorithm 1, we set the prescribed tolerance $\varepsilon=4.5\times10^{-5}$, and choose $\gamma=1.95$, $s=0.11$, $r_1=17+2\|\boldsymbol{X}_e\boldsymbol{\Lambda}_e\|_F^2$, $r_2=17+2\|\boldsymbol{X}_e\|_F^2$ and $t_1=t_2=1.001$. Algorithm 1 terminates after 159 iterations. Numerical results are reported in Table 1.

Table 1 Numerical results of Example 1

i	Err	$\lambda_i^{(\mathrm{err})}$	$\theta_i^{(\mathrm{err})}$
1		$1.056\,3\times10^{-6}$	$5.203\,5\times10^{-6}$
2	$7.226\,8\times10^{-6}$	$2.927\,4\times10^{-7}$	$3.965\,2\times10^{-6}$
3		$2.693\,2\times10^{-7}$	$2.437\,5\times10^{-6}$

The updated mass and stiffness matrices are obtained as follows

$$\boldsymbol{M}=\begin{bmatrix}1.000\,0&0.000\,0&0.000\,0&0.000\,0&0.000\,0\\0.000\,0&1.000\,0&0.000\,0&0.000\,0&0.000\,0\\0.000\,0&0.000\,0&1.000\,0&0.000\,0&0.000\,0\\0.000\,0&0.000\,0&0.000\,0&1.000\,0&0.000\,0\\0.000\,0&0.000\,0&0.000\,0&0.000\,0&1.000\,0\end{bmatrix}$$

$$\boldsymbol{K}=\begin{bmatrix}1.000\,0&-0.500\,0&0.000\,0&0.000\,0&0.000\,0\\-0.500\,0&1.000\,0&-0.500\,0&0.000\,0&0.000\,0\\0.000\,0&-0.500\,0&1.000\,0&-0.500\,0&0.000\,0\\0.000\,0&0.000\,0&-0.500\,0&1.000\,0&-0.500\,0\\0.000\,0&0.000\,0&0.000\,0&-0.500\,0&1.000\,0\end{bmatrix}$$

The updated mass and stiffness matrices $\boldsymbol{M}$ and $\boldsymbol{K}$ have the same zero/nonzero patterns as $\boldsymbol{M}_a$ and $\boldsymbol{K}_a$, respectively. It is easy to verify that $\boldsymbol{M}\geqslant0$ and $\boldsymbol{K}\geqslant0$. Table 1 shows that the updated matrices $\boldsymbol{M}$ and $\boldsymbol{K}$ satisfy the characteristic equation and the differences between the measured eigenpairs and the reproduced ones are very small.

The following two real-life models are built by Patran 2008 r2 and analyzed by Nastran[40].

Example 2[28] Consider a cantilever with one fixed end and a lumped mass on the other free end. The cross section of the cantilever is like "I" (Fig.2). The length and height of the cantilever are $L_1=1$ m and $L_2=0.05$ m, respectively. The geometric parameters of the cross section are $H=0.1$ m, $W_1=W_2=0.068$ m, $t=0.004\,5$ m, and $t_1=t_2=0.007\,6$ m. The elastic modulus is 2.0×10^{11} N/m^2, Poisson's ratio is 0.33, and the density is 7 800 kg/m^3. The lumped mass on the free end is $F=2$ kg. The cantilever is meshed into 40 nodes with 6 degrees of freedom by using finite element method. The 240×240 analytical mass and stiffness matrices $\hat{\boldsymbol{M}}$ and $\hat{\boldsymbol{K}}$ are obtained. $\hat{\boldsymbol{M}}$ has 122 nonzero entries, $\hat{\boldsymbol{K}}$ has 1 098 nonzero entries, and they have special zero/nonzero patterns.

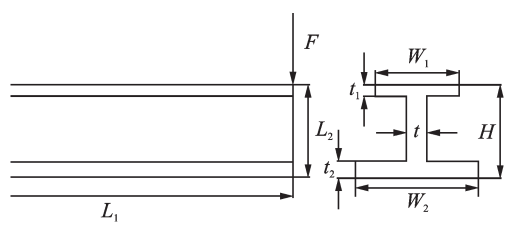

Fig.2 Cantilever with "I" cross section

In order to illustrate the effectiveness of Algorithm 1, we choose four lower order eigenpairs

$\left\{(\lambda_j, x_j)\right\}_{j=1}^{4}$ of the matrix pencil $(\hat{M}, \hat{K})$ as the measured eigendata, and set

$$M_a := \hat{M} + \mu R_M * \hat{M},\ K_a := \hat{K} + \mu R_K * \hat{K}$$

where $R_M = \begin{pmatrix} R_M^0 & 0 \\ 0 & 0 \end{pmatrix}$, $R_K = \begin{pmatrix} R_K^0 & 0 \\ 0 & 0 \end{pmatrix} \in \mathrm{R}^{240\times 240}$, R_M^0 and R_K^0 are 30×30 symmetric matrices whose entries are generated randomly and distributed uniformly within $[-1.0, 1.0]$, and μ is a perturbed parameter. For succinctness, we only report numerical results for the case where $\mu=0.001$. In this example, we set the prescribed tolerance $\varepsilon=5\times10^{-4}$, and choose $\gamma=1.58$, $s=0.5$, $r_1 = 21 + 2\left\|X_e \Lambda_e\right\|_F^2$, $r_2 = 21 + 2\left\|X_e\right\|_F^2$ and $t_1=t_2=1.1$. Using Algorithm 1, the perturbed mass and stiffness matrices are updated from the given eigendata. Algorithm 1 terminates after 2 110 iterations. Numerical results are listed in Table 2.

Table 2 Numerical results of Example 2

i	Err	$\lambda_i^{(\mathrm{err})}$	$\theta_i^{(\mathrm{err})}$
1		$1.932\ 6\times10^{-4}$	$3.844\ 8\times10^{-5}$
2	$3.838\ 2\times10^{-5}$	$2.577\ 7\times10^{-4}$	$1.229\ 4\times10^{-4}$
3		$1.100\ 1\times10^{-4}$	$1.695\ 9\times10^{-4}$
4		$5.640\ 3\times10^{-6}$	$8.399\ 1\times10^{-4}$

Table 2 shows that the updated matrices M and K satisfy the characteristic equation and the differences between the measured eigenpairs and the reproduced ones are very small. It is easy to verify that the updated matrices satisfy symmetry, positive semidefiniteness and sparsity simultaneously.

Example 3[28] The deflection of a plate acted on by a distributed load is considered as shown in Fig.3. The geometric and physical parameters of the plate are $h=0.01$ m, $L=1.2$ m, $w=0.6$ m, elastic modulus 7.0×10^{10} N/m^2, Poisson's ratio 0.33, and density 2 800 kg/m^3. The distributed load $F=$ 2 000 N/m^3 is rigidly supported at its two borderlines. Using finite element method, we mesh the plate into 150 rectangular grids, and obtain 1 008$\times$ 1 008 analytical mass and stiffness matrices $\hat{M}$ and $\hat{K}$ with special zero/nonzero patterns. There are 504 nonzero entries in $\hat{M}$ and 14 418 nonzero entries in $\hat{K}$.

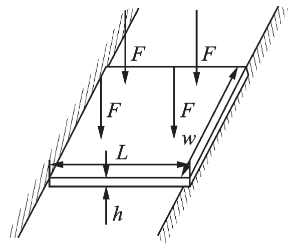

Fig.3 Plate with distributed load

We choose 20 lower order eigenpairs $\{(\lambda_j, x_j)\}_{j=1}^{20}$ of the matrix pencil $(\hat{M}, \hat{K})$ as the given eigendata, and set $M_a := \hat{M} + \mu R_M * \hat{M}, K_a := \hat{K} + \mu R_K * \hat{K}$, where $R_M = \begin{pmatrix} R_M^0 & 0 \\ 0 & 0 \end{pmatrix}$, $R_K = \begin{pmatrix} R_K^0 & 0 \\ 0 & 0 \end{pmatrix} \in \mathrm{R}^{1008\times 1008}$, R_M^0 and R_K^0 are 60×60 symmetric matrices whose entries are generated randomly and distributed uniformly within $[-1.0, 1.0]$, and $\mu=0.001$ is a perturbed parameter. Letting $\varepsilon = 1\times10^{-3}$, $\gamma=1.5$, $s=1.01$, $r_1 = 23 + 2\left\|X_e \Lambda_e\right\|_F^2$, $r_2 = 23 + 2\left\|X_e\right\|_F^2$ and $t_1=t_2=1.44$, and using Algorithm 1, we obtain the updated mass and stiffness matrices M and K after 3 636 iterations. Numerical results are given in Table 3.

It is easy to verify that the updated matrices are symmetric and positive semidefinite, and have the

Table 3 Numerical results of Example 3

i	Err	$\lambda_i^{(\mathrm{err})}$	$\theta_i^{(\mathrm{err})}$
1		$5.739\ 5\times10^{-4}$	$8.600\ 9\times10^{-4}$
2		$1.162\ 7\times10^{-4}$	$5.483\ 2\times10^{-4}$
3		$5.815\ 1\times10^{-4}$	$8.653\ 0\times10^{-4}$
4		$4.219\ 1\times10^{-5}$	0.002 4
5		$2.797\ 6\times10^{-4}$	$9.876\ 4\times10^{-4}$
6		$1.444\ 2\times10^{-4}$	0.001 7
7		$6.638\ 4\times10^{-5}$	$9.566\ 6\times10^{-4}$
8		$3.526\ 2\times10^{-4}$	0.002 5
9		0.001 5	0.001 6
10	$1.594\ 4\times10^{-4}$	$3.733\ 3\times10^{-4}$	$9.359\ 9\times10^{-4}$
11		$7.762\ 7\times10^{-5}$	$6.815\ 4\times10^{-4}$
12		$3.260\ 4\times10^{-4}$	0.002 1
13		0.001 0	0.001 8
14		$6.955\ 5\times10^{-4}$	0.002 9
15		0.002 1	0.001 2
16		0.001 7	0.001 8
17		$7.317\ 1\times10^{-4}$	0.001 1
18		0.002 5	0.001 3
19		0.002 3	0.010 5
10		0.001 9	0.004 9

same zero/nonzero patterns as $\hat{M}$ and $\hat{K}$. Table 3 shows that the updated matrices $\boldsymbol{M}$ and $\boldsymbol{K}$ satisfy the characteristic equation and the differences between the given eigenpairs and the reproduced ones are very small.

5 Conclusions

In this paper, we consider the problem of correcting simultaneously mass and stiffness matrices of finite element model of undamped structural systems using vibration tests, and develop a new analytical model updating method on the basis of the optimal matrix pencil approximation and the proximal point method for solving variational inequalities. In this method, the desired matrix properties, including satisfaction of the dynamic equation, symmetry, positive semidefiniteness and sparsity or connectivity, are imposed, thus preserving the physical and geometric configuration of the analytical model. Numerical examples demonstrate that the new model updating method is effective.

References

[1] STEWART G W. Matrix algorithms, Vol II: Eigensystems[M]. Philadelphia: SIAM, 2001.

[2] FRISWEEL M I, MOTTERSHEAD J E. Finite element model updating in structural dynamics[M]. Dordrecht: Kluwer Academic Publishers, 1995.

[3] ZHANG D W, WEI F S. Model updating and damage detection[M]. Beijing: Science Press, 1999.

[4] BARUCH M. Optimization procedure to correct stiffness and flexibility matrices using vibration tests[J]. AIAA Journal, 1978, 16(11): 1208-1210.

[5] WEI F S. Stiffness matrix correction from incomplete test data[J]. AIAA Journal, 1980, 18(10): 1274-1275.

[6] DAI H. Stiffness matrix correction using test data[J]. Acta Aeronautica et Astronautica Sinica, 1994, 15(9): 1091-1094.

[7] KENIGSBUCH R, HALEVI Y. Model updating in structural dynamics: A generalised reference basis approach[J]. Mechanical Systems and Signal Processing, 1998, 12(1): 75-90.

[8] KABE A M. Stiffness matrix adjustment using mode data[J]. AIAA Journal, 1985, 23(9): 1431-1436.

[9] SAKO B H, KABE A M. Direct least-squares formulation of a stiffness adjustment method[J]. AIAA Journal, 2005, 43(2): 413-419.

[10] DAI H. On the symmetric solutions of linear matrix equations[J]. Linear Algebra and Its Applications, 1990, 131: 1-7.

[11] DAI H. The stability of solutions for inverse problems of symmetric matrices[J]. Journal of Nanjing University of Aeronautics & Astronautics, 1994, 26(1): 133-139. (in Chinese)

[12] LI S, FENG T H, FAN X J. An updating method for local model errors[J]. Transactions of Nanjing University of Aeronautics & Astronautics, 1995, 12(2): 129-133.

[13] YUAN Q. Dual approaches to finite element model updating[J]. Journal of Computational and Applied Mathematics, 2012, 236(7): 1851-1861.

[14] YUAN Q. Matrix linear variational inequality approach for finite element model updating[J]. Mechanical Systems and Signal Processing, 2012, 28: 507-516.

[15] YUAN Q. Proximal-point method for finite element model updating problem[J]. Mechanical Systems and Signal Processing, 2013, 34: 47-56.

[16] BERMAN A. Mass matrix correction using an incomplete set of measured modes[J]. AIAA Journal, 1979, 17(10): 1147-1148.

[17] ZHANG D W, ZHANG L M. Matrix transformation method for updating dynamic model[J]. AIAA Journal, 1992, 30(5): 1440-1443.

[18] LEE E T, RAHMATALLA S, EUN H C. Estimation of parameter matrices based on measured data[J]. Applied Mathematical Modelling, 2011, 35(10): 4816-4823.

[19] WEI F S, ZHANG D W. Mass matrix modification using element correction method[J]. AIAA Journal, 1989, 27(1): 119-121.

[20] CHA P D. Correcting system matrices using the orthogonality conditions of distinct measured modes[J]. AIAA Journal, 2000, 38(4): 730-732.

[21] DAI H, WEI W. Mass matrix correction of finite element model using measured test data[J]. Journal of Nanjing University of Aeronautics & Astronautics, 2017, 49(5): 606-611. (in Chinese)

[22] BARUCH M. Optimal correction of mass and stiffness matrices using measured modes[J]. AIAA Journal, 1982, 20(11): 1623-1626.

[23] BERMAN A, NAGY E J. Improvement of a large analytical model using test data[J]. AIAA Journal, 1983, 21(8): 1168-1173.

[24] CHA P D, GU W. Model updating using an incomplete set of experimental modes[J]. Journal of Sound and Vibration, 2000, 233(4): 587-600.

[25] WANG K, YANG J. Dynamical model updating based on modal tests with changed structure[J].

Transactions of Nanjing University of Aeronautics & Astronautics, 2014, 31(1): 56-63.

[26] DAI H. Optimal approximation of real symmetric matrix pencil under spectral restriction[J]. Numerical Mathematics—Journal of Chinese Universities, 1990, 12(2): 177-187.

[27] WEI F S. Structural dynamic model improvement using vibration test data[J]. AIAA Journal, 1990, 28 (1): 175-177.

[28] YUAN Q, DAI H. The matrix pencil nearness problem in structural dynamic model updating[J]. Journal of Engineering Mathematics, 2015, 93(1): 131-143.

[29] WANG K, DAI H. Alternating projection method for matrix pencil nearness problem[J]. Communication on Applied Mathematics and Computation, 2017, 31 (2): 163-175.

[30] RAKSHIT S, KHARE S R. Symmetric band structure preserving finite element model updating with no spillover[J]. Mechanical Systems and Signal Processing, 2019, 116: 415-431.

[31] NOCEDAL J, WRIGHT S J. Numerical optimization[M]. Berlin: Springer-Verlag, 1999.

[32] YING J Q, WEI Q L. Nonlinear programming and its theory[M]. Beijing: Renmin University of China Press, 1994.

[33] MARTINET B. Regularisation d'inequations variationnelles par approximations succesives[J]. ESAIM: Mathematical Modelling and Numerical Analysis, 1970, 4: 154-159.

[34] ROCKAFELLAR R T. Monotone operators and the proximal point algorithm[J]. SIAM Journal on Control and Optimization, 1976, 14(5): 877-898.

[35] BURACHIK R S, IUSEM A N. A generalized proximal point algorithm for the variational inequality problem in a Hilbert space[J]. SIAM Journal on Optimization, 1998, 8(1): 197-216.

[36] HE B S, Fu X L, JIANG Z K. Proximal-point algorithm using a linear proximal term[J]. Journal of Optimization Theory and Applications, 2009, 141(2): 299-319.

[37] HIGHAM N J. Computing a nearest symmetric positive semidefinite matrix[J]. Linear Algebra and Its Applications, 1988, 103: 103-118.

[38] HE B S, SHEN Y. On the convergence rate of customized proximal point algorithm for convex optimization and saddle-point problem[J]. Science China Mathematics, 2012, 42(5): 515-525.

[39] BLUM E, OETTLI W. Mathematische optimierung, econometrics and operations research XX[M]. Berlin: Springer-Verlag, 1975.

[40] MA A J. Finite element analysis using Patran and Nastran[M]. Beijing: Tsinghua University Press, 2005.

Acknowledgement The work was supported by the National Natural Science Foundation of China (No.11571171).

Author Prof. **DAI Hua** received the B.S. degree and M.S. degree in computational mathematics from Nanjing University of Aeronautics and Astronautics (NUAA) in 1982 and 1986, respectively, and Ph.D. degree in computational mathematics from Nanjing University in 1988. In Dec. 1988, he joined the Department of Mathematics, NUAA, Nanjing, China. Prof. DAI is engaged in the research of numerical algebra, scientific computing, inverse problem and so on. His research interest includes numerical methods for solving large-scale linear systems, algebraic eigenvalue problems and discrete ill-posed problems, sensitivity analysis, finite element model updating and partial eigenvalue assignment of linear systems.

Author contributions Prof. **DAI Hua** designed the study, revised and modified the manuscript. Mr. **WANG Kangkang** conducted the analysis and wrote the manuscript. All authors commented on the manuscript draft and approved the submission.

Competing interests The authors declare no competing interests.

(Production Editor: ZHANG Huangqun)

同时修正有限元模型质量和刚度矩阵的邻近点型方法

戴 华,王康康

(南京航空航天大学理学院,南京 211106,中国)

摘要:研究了由振动试验数据同时修正无阻尼结构系统有限元模型的质量和刚度矩阵。期望的矩阵性质包括满足特征方程、对称性、半正定性和稀疏性作为约束条件形成矩阵束最佳逼近问题。利用部分Lagrangian乘子法,将非线性约束优化问题转化为一个等价的矩阵线性变分不等式,提出了求解该矩阵线性变分不等式的一个邻近点型方法,并分析其全局收敛性。最后用数值结果说明了本文方法的性能和应用。

关键词:模型修正;邻近点方法;矩阵束最佳逼近;矩阵线性变分不等式